CHAPTER THREE

Activity-based ATP analog probes for bacterial histidine kinases

Hannah K. Lembke[a] **and Erin E. Carlson**[a,b,c,d,*]

[a]Department of Chemistry, University of Minnesota, Minneapolis, MN, United States
[b]Department of Medicinal Chemistry, University of Minnesota, Minneapolis, MN, United States
[c]Department of Biochemistry, Molecular Biology, and Biophysics, University of Minnesota, Minneapolis, MN, United States
[d]Department of Pharmacology, University of Minnesota, Minneapolis, MN, United States
*Corresponding author: e-mail address: carlsone@umn.edu

Contents

Methods in Enzymology, Volume 664
ISSN 0076-6879
https://doi.org/10.1016/bs.mie.2022.01.003

Abstract

Histidine kinases (HKs) are sensor proteins found ubiquitously in prokaryotes. They are the first protein in two-component systems (TCSs), signaling pathways that respond to a myriad of environmental stimuli. TCSs are typically comprised of a HK and its cognate response regulator (RR) which often acts as a transcription factor. RRs will bind DNA and ultimately lead to a cellular response. These cellular outputs vary widely, but HKs are particularly interesting as they are tied to antibiotic resistance and virulence pathways in pathogenic bacteria, making them promising drug targets. We anticipate that HK inhibitors could serve as either standalone antibiotics or antivirulence therapies. Additionally, while the cellular response mediated by the HKs is often well-characterized, very little is known about which stimuli trigger the sensor kinase to begin the phosphorylation cascade. Studying HK activity and enrichment of active HKs through activity-based protein profiling will enable these stimuli to be elucidated, filling this fundamental gap in knowledge. Here, we describe methods to evaluate the potency of putative HK inhibitors in addition to methods to calculate kinetic parameters of various activity-based probes designed for the HKs.

1. Introduction

Two-component systems (TCSs) are ubiquitous protein signaling pathways found mainly in prokaryotes and are crucial for bacteria to respond to environmental stimuli. Bacteria generally possess 20–100 unique TCSs, demonstrating the range they have in responding to the continually changing environments that bacteria face (Stock, Robinson, & Goudreau, 2000). TCSs are implicated in motility (CheA, CheY) (Cannistraro, Glekas, Rao, & Ordal, 2011; Li & Hazelbauer, 2004; Surette et al., 1996), as well as sensing and responding to temperature changes (DesK) (Albanesi et al., 2009), alterations in the pH of their surroundings (ArsS) (Muller, Gotz, & Beier, 2009), and of particular interest, the presence of antibiotics (PmrA/VbrK) (Dorr et al., 2016; Francis, Stevenson, & Porter, 2017). In addition to these pathways, TCSs are implicated in other virulence mechanisms such as biofilm formation (Bhagirath et al., 2019), toxin production (Francis et al., 2017) and quorum sensing (Gotoh et al., 2010), which lead to increased infectivity in pathogenic bacteria. TCSs are aptly named as most of these systems are comprised of two proteins, a sensor histidine kinase (HK) and its cognate response regulator (RR) (Stock et al., 2000). A signaling cascade begins when a stimulus activates the sensory domain (SD) of the HK triggering a dimerization event, followed by binding of adenosine triphosphate (ATP), in the catalytic ATP binding (CA) domain. The CA domain is connected to the dimerization and histidine phosphorylation (DHp) domain through a flexible loop. Once ATP is bound, a confirmational

change occurs and the CA domain closes onto a conserved histidine residue located on the DHp domain, autophosphorylating it (Casino, Miguel-Romero, & Marina, 2014).

Next, a phosphotransfer takes place between the HK and a conserved aspartate residue on the RR. RRs typically act as transcription factors, binding directly with DNA to alter gene expression (Fig. 1) (Hazelbauer & Lai, 2010). Inhibition of these systems is of particular interest, since downregulating these pathways can lead to decreased pathogenicity and/or a greater susceptibility to host immune response (Beier & Gross, 2006; Bem et al., 2015; Bhagirath et al., 2019; Francis et al., 2017; Gotoh et al., 2010). HKs are particularly intriguing therapeutic targets for various reasons. First, the CA domain has a high degree of homology throughout distinct HKs both within an organism and between organisms, which could enable the generation of pan-HK inhibitors. In addition to their absence in mammals, HKs contain discrete structures relative to mammalians kinases. Specifically, the Bergerat fold found in the CA domain of the HK is unique to a small family of proteins not including mammalian kinases, circumventing potential toxicity for human therapy (Bem et al., 2015). HK inhibitors have the potential to act as stand-alone therapeutics, in addition to having synergistic effects with current day antibiotics.

To identify potent inhibitors, the activity of the HKs must be measured in vitro. Studying the activity of the HKs is difficult due to the intrinsic

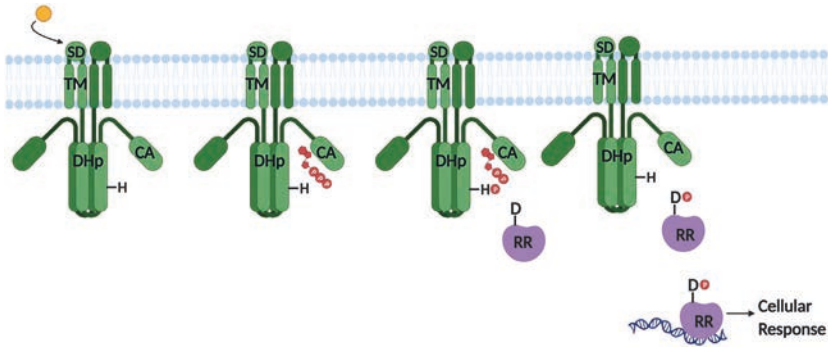

Fig. 1 Overview of two-component systems. Signaling cascade shows activation of TCS, first a signal binds to the sensory domain (SD), then ATP binds to the catalytic and ATP-binding domain (CA), the HK autophosphorylates on a conserved histidine present on the dimerization and histidine phosphorylation domain (DHp). A phosphotransfer takes place between the conserved histidine to a conserved aspartate on the cognate response regulator, which then binds DNA and leads to a specific cellular response. TM = transmembrane domain.

instability of the phosphohistidine (pHis) species formed in the DHp domain (Kee & Muir, 2012). The pHis modification contains a phosphoramidate bond, which is highly acid-sensitive and labile even under neutral conditions with a ΔG of -12 to $-13\,kcal\,mol^{-1}$ in comparison to serine, threonine or tyrosine kinases commonly found in mammals, which when phosphorylated have ΔG values of -6.5 to $-9.5\,kcal\,mol^{-1}$ (Kee & Muir, 2012). To increase the stability of the pHis modification, ATPγS was utilized instead of native ATP. The sulfur atom on the terminal phosphate lends stability to the thio-pHis species due to its decreased electronegativity (Makwana, Muimo, & Jackson, 2018). Radioactive ATPγS has been utilized to determine the activity of HKs in vitro, however, radioactive work can be expensive and dangerous. To combat these problems, while maintaining sensitivity when labeling the HKs, we developed the first fluorescent, activity-based ATP analog, BODIPY-FL-ATPγS (B-ATPγS; Fig. 2A) (Wilke, Francis, & Carlson, 2012). B-ATPγS also harnesses the stability given by a terminal sulfur atom, in addition to utilizing a convenient fluorescent readout compared to laborious radioactive work. The development of this activity-based probe (ABP) enabled not only the ability to distinguish how much an inhibitor mitigates HK activity but serves as an additional tool to study the autophosphorylation of HKs and other ATP-binding proteins (Espinasse, Lembke, Cao, & Carlson, 2020; Espinasse, Wen, Goodpaster, & Carlson, 2020; Goswami, Espinasse, & Carlson, 2018).

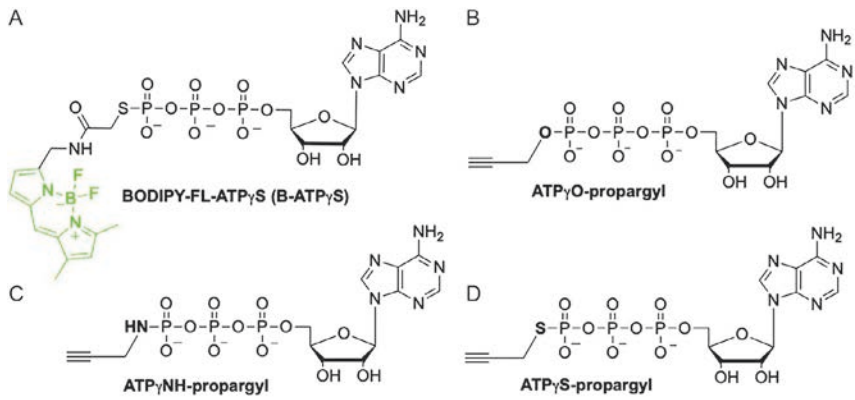

Fig. 2 ATP activity-based probe structures. (A) BODIPY-FL-ATPγS, original activity-based probes developed for labeling active HKs, BODIPY fluorophore highlighted in green. (B) ATPγO-propargyl, terminal oxygen linked to propargyl group bolded. (C) ATPγNH-propargyl, terminal nitrogen atom linked to propargyl group is bolded. (D) ATPγS-propargyl, terminal sulfur linked to propargyl group bolded.

2. ATP analog activity-based probes

Activity-based protein profiling is a strategy that has been utilized for several decades to study the activity of enzymes through applying active-site directed chemical probes known as activity-based probes (ABPs). ABPs are comprized of three moieties, including a functional group that reacts in a mechanism-dependent manner with the active site of an enzyme, also commonly referred to as a warhead (Heal, Dang, & Tate, 2011). Warheads are often electrophilic, such as the case for β-lactone probes for penicillin-binding proteins (Sharifzadeh, Shirley, & Carlson, 2019), however, recently nucleophilic warheads have been applied to target electrophilic post-translational modifications on proteins in eukaryotic cells (Matthews et al., 2017). The second component is a reporter tag such as fluorophore or bioorthogonal handle. Tags can also be moieties like biotin, which are useful in protein pull-down assays to enrich labeled proteins from a sample (Zanon, Lewald, & Hacker, 2020). Lastly, there is a linker between the reporter and the functional group. Linkers can range anywhere from alkyl chains of varying lengths to hydrophilic groups such as repeating units of polyethylene glycol (PEG) (Fang et al., 2021). ABPs are typically designed so that the reactive functional group is specific for a distinct protein or class of proteins. ABPs are broadly applicable to many fields of study but have found particular use in chemical proteomics, where capture of active enzymes by an ABP enables further classification of these modified proteins with downstream analysis. This methodology has elucidated several putative proteins in pathways of interest and further discussion of these is outside the scope of this chapter and the reader is referred to additional examples from Fang et al. (2021) and Wang et al. (2018). Our ABPs utilized the native substrate of kinases, ATP, and while ATP is a common substrate found in cells, the assays described herein utilize pure protein to enable a proof-of-concept experiments. However, as is the case with other generic electrophilic scaffolds, such as the fluorophosphonates (Shamshurin, Krokhin, Levin, Sparling, & Wilkins, 2014), our ATP-based ABPs can be used with cellular lysates or *in cellulo* to label ATP-binding enzymes, including HKs.

2.1 Suite of ATP-based probes

The ABPs that we designed contain ATP as the core with a γ-phosphate that reacts with a histidine of an active HK. Our original probe, B-ATPγS,

contains a BODIPY fluorophore as a reporter group, and a short, alkyl linker connecting these two groups (Wilke et al., 2012).

We have further developed this work by utilizing a suite of ATP-propargyl probes, which enables the use of the common bioorthogonal copper(I)-catalyzed alkyne azide cycloaddition (CuAAC) reaction (Dommerholt et al., 2014; Hong, Presolski, Ma, & Finn, 2009; Wright & Sieber, 2016). These were compared for their kinetic properties as well as labeling efficiencies (Espinasse, Wen, et al., 2020). These probes differ only in their terminal atom linking the propargyl group to the ATP core. The first contains the native oxygen (ATPγO-propargyl, Fig. 2B), the second, a nitrogen (ATPγNH-propargyl, Fig. 2C), and finally the third a sulfur (ATPγS-propargyl, Fig. 2D). Benefits of using the alkyne-containing probes include decreased non-specific interactions between the fluorophore and protein of interest, as well as the ability to append any desired read-out tag. While these probes can be applied to an extensive array of proteins, our focus is on the HKs. We have demonstrated the versatility of these probes by both validating HK inhibitor hits and determining kinetic parameters for all three proparygl probes (Fig. 2B–D**)** (Espinasse, Wen, et al., 2020).

2.2 Activity assay with putative HK inhibitors

From a fluorescence polarization screen completed by Wilke et al., 115 HK hits were identified from a 53,311 compound library (Wilke, Francis, & Carlson, 2015). One of these hits was riluzole, an FDA approved drug used for the treatment of Amyotrophic Lateral Sclerosis (ALS) (Coleman et al., 2015). We further evaluated the efficacy of a small library based on the benzothioazole scaffold found in riluzole and several other hits (Goswami et al., 2018). Each inhibitor (Rilu-4 shown in Fig. 3B) was incubated with the constitutively active model HK, HK853, followed by B-ATPγS to label any free and active protein. The reaction was then quenched with loading buffer and run on a polyacrylamide gel. From the integrated band densities of fluorophore labeling, the half maximal inhibitory concentration (IC_{50} value) was calculated (Fig. 3).

2.3 Concentration-dependent kinetics assay with suite of ATP propargyl probes

The comparison of kinetic properties between a native substrate and chemical probes used to evaluate the activity of proteins is critical to understanding not only how this probe may be disrupting the system but can also yield

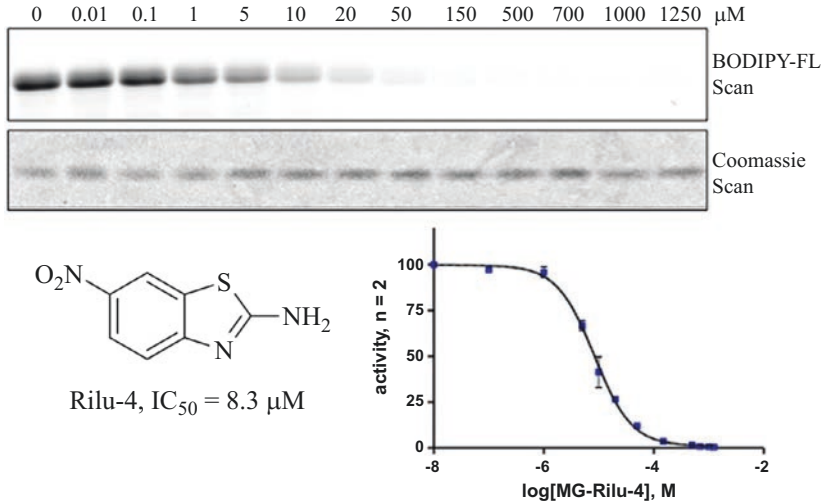

Fig. 3 Results from activity-based assay with Rilu-4 inhibitor. (A) Gel from activity assay with HK853 incubated with Rilu-4 and then labeled with B-ATPγS. (B) Rilu-4 molecular structure with its corresponding IC_{50} value. (C) IC_{50} curve for Rilu-4 inhibitor. *Modified from Goswami, M., Espinasse, A., Carlson, E. E. (2018). Disarming the virulence arsenal of* Pseudomonas aeruginosa *by blocking two-component system signaling.* Chemical Science, 10, *7332–7337. https://doi.org/10.1039/C8SC02496K.*

information about how to develop future chemical probes. For histidine phosphorylation, the lability of the pHis modification is an inherent liability. However, by designing chemical probes to yield more stable phosphorylation products (i.e., terminal sulfur compared to a terminal oxygen) we can improve the tools utilized to study these systems. We sought to determine the kinetic parameter for our suite of propargyl probes, including the catalytic efficiency (k_{cat}) and binding affinity (K_m). Using a concentration-dependent kinetics assay instead of a more traditional time-dependent kinetics assay enables kinetic parameters to be measured without having to quench reactions across various time points, especially in highly efficient proteins where enzyme saturation occurs rapidly. Instead, by using various concentrations and measuring the amount of modified pHis species generated at a single timepoint, Espinasse et al. determined the binding affinity for each probe (Fig. 4A). The enzyme displayed the best affinity for ATPγO-propargyl (Probe O, Fig. 4B) at 4.8 μM, followed by ATPγNH-propargyl (Probe N, Fig. 4B) at 6.9 μM, and ATPγS-propargyl (Probe S, Fig. 4B) at 29 μM. Additional calculations were performed to determine the apparent turnover (k_{cat}) and catalytic efficiency values for each probe (k_{cat}/k_m), with

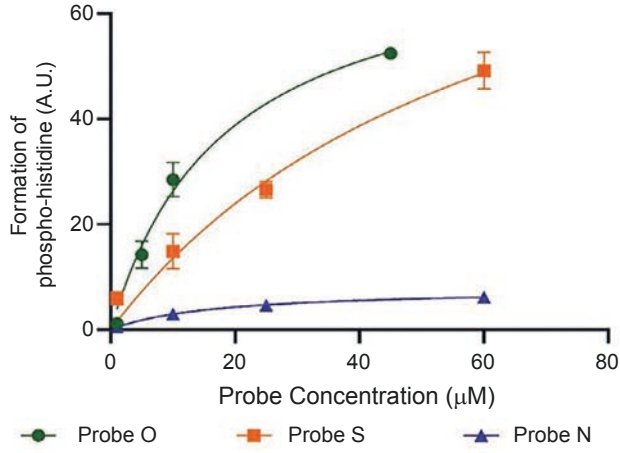

Probe	Binding Affinity K_m (μM)	Turnover Apparent K_{cm} (s^{-1})	Catalytic Efficiency Apparent K_{cm}/K_m ($M^{-1}.s^{-1}$)[1]
Probe O	4.8 ± 1.2	1.5 ± 0.1	0.31 (100%)
Probe S	29 ± 12	2.1 ± 0.6	0.070 (22%)
Probe N	6.9 ± 3.3	0.15 ± 0.03	0.022 (7%)

Fig. 4 Concentration-dependent kinetics assay with ATP propargyl probes. Top. Curves from gel-based kinetics assay. Bottom. Calculated kinetics parameters. *Modified from Espinasse, A., Wen, X., Goodpaster, J. D., Carlson, E. E. (2020). Mechanistic studies of bio-orthogonal ATP analogues for assessment of histidine kinase autophosphorylation.* ACS Chemical Biology, 15, *1252–1260. https://doi.org/10.1021/acschembio9b01024*.

ATPγS-propargyl and ATP-propargyl being superior to ATPγNH-propargyl. Since these probes alone do not give a directly detectable readout, such as fluorescence or radioactivity, only apparent values can be obtained.

3. Gel-based activity assays

3.1 Equipment

1. Genesys 30 Visible Spectrophotometer (or similar model)
2. Plastic 17 × 100 mm culture tubes (VWR, cat #60818-667)
3. Micropipettors
4. Micropipette tips

5. 1.5 mL microcentrifuge tubes
6. Incubator
7. Typhoon 9210 Gel Scanner (or similar model) with the following filters: Coomassie, ex/em 532 nm/570 nm ±20 nm, BODIPY, ex/em 504 nm/514 nm ±20 nm, TAMRA, ex/em 542 nm/568 nm ± 20 nm, Silver Stain or equivalent
8. Gel Electrophoresis Rig
9. Shaker/Incubator
10. Gel Rotator
11. Bench Top Centrifuge
12. Bench Top Vortex mixer
13. NanoDrop 1000 Spectrophotometer (Thermo Fisher Scientific)
14. Wand Sonifier (Branson)
15. ÄKTA FPLC (GE)
16. ImageJ software (NIH) for gel data analysis

3.2 Materials

1. *E. coli* BL21 pHis parallel HK853 cells (MW of HK853: 32,468 g/mol, Molar absorptivity of HK853: 27,390 M^{-1} cm^{-1})
2. LB Media (Sigma, powder, cat #L3022)
3. Agar (Sigma, powder, cat #A1296)
4. Ampicillin Sodium Salt
5. Isopropylthio-β-galactoside (IPTG)
6. EDTA Tablet (Roche, cat #04693159001)
7. DNase
8. Ni-NTA Buffer A (50 mM Tris, 1 M NaCl, 2 mM β-mercaptoethanol, 5 mM imidazole, 100 mM glycerol, pH 7.6)
9. Ni-NTA Buffer B (50 mM Tris, 500 mM NaCl, 100 mM glycerol, 2 mM β-mercaptoethanol, 1 M imidazole, pH 8)
10. Storage Buffer (50 mM Tris, 500 mM NaCl, 200 mM glycerol, 2 mM β-mercaptoethanol, pH 7.6)
11. Reaction Buffer (50 mM Tris-HCl, 200 mM KCl, 5 mM $MgCl_2$, pH 7.8)
12. Ambicon 30 kDa MW Spin Filters (Millipore, cat #PR05120)
13. 0.22 μM PES syringe filters
14. DMSO
15. Inhibitors
16. ATPγS BODIPY FL (ThermoFisher, cat# A22184)

17. Triton X-100
18. 10% Tris polyacrylamide gels
19. 4 × Loading Buffer [200 mM Tris-HCl, 400 mM dithiothreitol (DTT), 8% (*w*/*v*) Sodium dodecyl sulfate (SDS), 0.2% (w/v) bromophenol blue, 40% (*v*/v) glycerol, pH 6.8]
20. BenchMark Fluorescent Protein Standard (Invitrogen, cat# LC5928)
21. 10 × Tris-glycine SDS running buffer [144.0 g/L glycine, 30.0 g/L Tris, 10.0 g/L sodium dodecyl sulfate (SDS); pH 8.3]
22. Coomassie brilliant blue R-250 staining solution (Bio-Rad, cat #1610436)
23. Gel-destaining solution (40% v/v acetic acid, 10% v/v methanol)

3.3 Protocols

3.3.1 Protein overexpression and purification

1. Frozen glycerol stocks of *E. coli BL21* with a pHis-parallel 1 vector containing the gene corresponding to the cytosolic portion of HK853 (Marina, Waldburger, & Hendrickson, 2005) were spread onto 100 μg/mL ampicillin LB agar plate using a sterile inoculation loop. Plates were grown overnight at 37 °C
2. A single colony was selected from the LB agar plate and inoculated into 5 mL of LB broth with 100 μg/mL ampicillin and grown overnight at 37 °C and 220 RPM
3. The overnight culture was added to 1 L of fresh LB media with 100 μg/mL ampicillin and grown to an OD_{600} of ~0.5 at 37 °C and 220 RPM. Aliquots of this culture were placed into sterile cuvettes and read in a nanodrop spectrophotometer until the desired OD_{600} was reached
4. The culture was induced with 0.22 mM IPTG at 20 °C at 220 RPM overnight (~16 h) and then spun down at 8000 *g* for 30 min at 4 °C. The supernatant was removed, and cell pellet frozen at −80 °C. (*Stopping point-pellet can be stored at −80 °C until ready for lysis, up to many months*)
5. Cells were removed from storage at −80 °C and thawed on ice. Once thawed, the cell pellet was resuspended in 30 mL of lysis buffer (Buffer A) and transferred to a glass homogenizer with 1 EDTA free tablet (Roche) and 10 μg/mL DNAse. The container with the cell pellet was washed with an additional 10 mL of lysis buffer, which was then added to the homogenizer

6. Cells were homogenized by hand (10 ×) and the resulting material placed into a sterile falcon tube submerged in ice and lysed with a Branson wand sonifier for 15 s on/30 s off for 15 min total on time at 30% A
7. Lysate was spun down at 14000 *g* for 30 min at 4 °C
8. Lysate was clarified with a 0.22 μM PES syringe filter. (*Stopping Point-freeze clarified lysate at −80 °C until ready for purification*)
9. Filtered lysate (~40 mL) was purified at 4 °C on a Nickel affinity (Ni-NTA) column using a gradient of 0–100% Buffer B over 20 min. Elution of HK853 was monitored at 215 nm and occurred around 20% Buffer B
10. The purified protein was collected, concentrated with 30 kDa Ambicon filters, and purified on a 75/100 Superdex size exclusion column in storage buffer (50 mM Tris, 500 mM NaCl, 200 mM glycerol, 2 mM β-mercaptoethanol) over 120 min
11. Fractions containing protein were concentrated with 30 kDa Ambicon filters, the protein concentration measured by Nanodrop at 280 nm, and frozen in aliquots to avoid repeated freeze-thaw cycles during use (−80 °C)

3.3.2 Activity assay (IC_{50} assay)

1. Stock solutions of the inhibitor(s) were generated in DMSO (25 mM)
2. Dilution series in Table 1 used to make stock solutions of inhibitors varying from 0.01 to 1250 μM
3. Protein was thawed on ice and pipetted into a 30 kDa filter fitted into a microcentrifuge tube to exchange protein storage buffer to protein reaction buffer (amount needed will depend on frozen protein stock concentration and how much protein solution is needed for assays)
4. Reaction buffer was added (400 μL) and samples were centrifuge for 5 min at 15,000*g*
5. Flow-through was discarded and this was repeated two additional times
6. Filter was placed upside down into a fresh tube and centrifuged for 2 min at 15,000*g*
7. Concentration of the protein was measured at 280 nm (or through equivalent assay) and diluted to reach 0.48 μM with reaction buffer
   7.1. These stock solutions should be used within 24 h to maintain consistent activity of the protein
8. Triton X-100 was added to reach a final concentration of 0.1% *v*/v and the protein solution was filtered through a 0.2 μM filter to remove of particulates that may interfere with the assay

Table 1 Inhibitor working stock dilution series for gel-based activity assay.

Previous working stock (μM)	DMSO to add (μL)	Previous working stock (μL)	Working inhibitor stock (μM)	Final [inhibitor] (μM)
2	10.80	1.20	0.2	0.01
20	10.80	1.20	2	0.1
100	9.60	2.40	20	1
200	6.00	6.00	100	5
400	6.00	6.00	200	10
1000	7.20	4.80	400	20
3000	8.00	4.00	1000	50
10,000	8.40	3.60	3000	150
25,000	7.20	4.80	10,000	500
25,000	2.20	2.80	14,000	700
25,000	1.00	4.00	20,000	1000
25,000	0.00	5.00	25,000	1250

9. Protein solution (23.75 μL) was added to each sample tube for a final concentration of 0.46 μM in 25 μL total volume
10. DMSO or the appropriate stock solution of inhibitor designated in Table 1 (1.25 μL) were added into the microcentrifuge tubes and briefly vortexed
11. Incubated protein and inhibitor for 30 min at RT
12. During this incubation, prepare a 50 μM solution of B-ATPγS probe in MilliQ water
13. After incubation is complete, B-ATPγS was added (1.25 μL) to each sample, vortexed, and briefly centrifuged
14. Samples incubated in the dark at RT for 1 h
15. Reaction quenched by adding 8.6 μL of 4 × loading buffer to each sample (*Stopping Point-freeze samples in loading buffer at − 20 °C for several days as needed*)
16. Add 10 μL of each sample to a 10% polyacrylamide gel and run at 180 V for 1 h in the dark on ice (Fig. 5)
17. Gel was removed from cassette and rinsed 3 × with MilliQ water

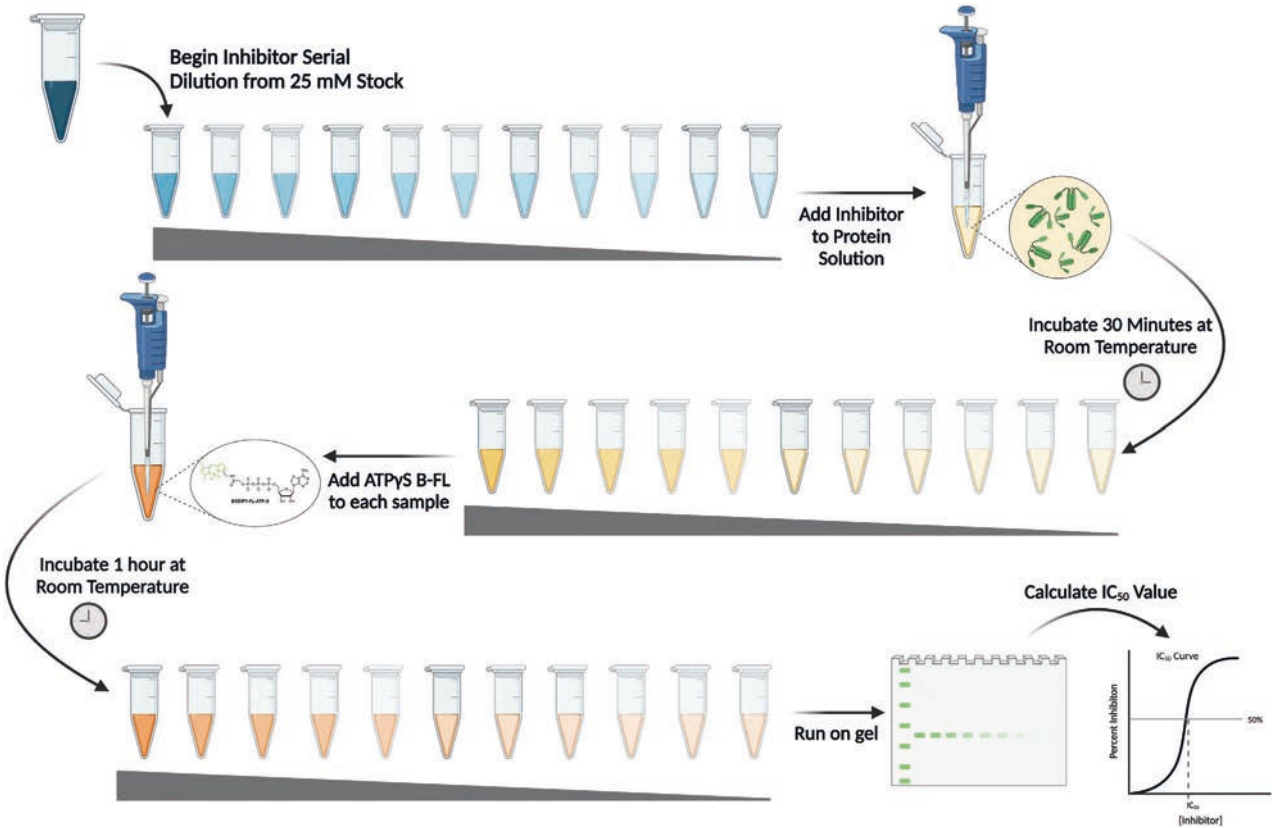

Fig. 5 Schematic of activity assay. Dilution series of inhibitor is added to protein solution in microcentrifuge tubes. Incubation occurs for 30 min, then ATPγS B-FL is added and incubated for a further hour in the dark. Samples quenched with loading buffer and run on a 10% polyacrylamide gel to be quantitatively analyzed in ImageJ with data work-up performed in Graphpad Prism.

18. Gel was scanned in the BODIPY (ex/em 504 nm/514 nm ± 20 nm) or equivalent channel
19. Gel was subjected to 40 mL of Coomassie solution, microwaved for 1 min, and rotated on gel shaker for 30 min
20. Solution was decanted and gel rinsed gel 3 × with MilliQ water
21. Gel destaining solution (40 mL) was added and microwaved for 1 min, followed by incubation overnight. Destained gel was scanned in the Coomassie channel (ex/em 532 nm/570 nm ± 20 nm)

3.4 Analysis

3.4.1 ImageJ quantification

1. Load fluorescent scan of gel and Coomassie scan of gel into ImageJ (NIH, 2021)
2. Click "Process" button, then at the bottom select "Subtract Background"
3. Under "Image," select "Adjust" then "Brightness/Contrast." Shift the contrast using the pop-out box until gel bands are clearly visible but not oversaturating the image
4. Select the "rectangle" button in the far-left corner of ImageJ and create a box around the gel that excludes any excess gel or lanes that will not be processed
5. Select "Image," then "Crop" and exclude anything but the lanes being evaluated. You will now have a cropped, background subtracted gel image to work with
6. Draw a new rectangle over a single protein band within the gel. Under the "Analyze" menu select "Measure." A new box pops up labeled "Results," with the following records: Sample number (in the order measured), area of rectangle, Mean value, Minimum (min) and Maximum value (max), the integrated density and raw integrated density. Make note of the area of this rectangle, as it *must remain the same* to compare any band density moving forward
7. Move cursor until an arrow pops up (not a cross, this will draw a new rectangle and not a finger, this will change the size of the current rectangle)
8. Slid the rectangle directly up from measured band and measure this value to serve as the background for that gel lane
9. Repeat steps 7–8 for each sample band and background, recording the order in which each sample was measured

10. Subtract the lane-specific blank integrated density for each sample from the sample's measured integrated density to collect the corrected integrated densities

3.4.2 Dose response curve

1. Divide the corrected integrated densities for each inhibitor concentration by the DMSO control to get percent inhibition for the specified inhibitor concentration
2. Repeat for each biological replicate of the activity assay and calculate the standard deviations for each sample
3. Use Graphpad Prism 8.0 (or similar software) to plot each log [inhibitor] with its corresponding percent inhibition on the y-axis, which gives an IC_{50} curve and include the previously calculated standard deviations as error bars
4. Calculate IC_{50} values using Graphpad Prism 8.0 by entering biological replicate values into two tables. The x value is the log [inhibitor], the y value is the percent inhibition at the corresponding [inhibitor]
5. Select "New Analysis" and scroll to "Nonlinear Regression (curve fit)" under the "XY Analyses" title
6. Select "log(inhibitor) vs response" then "Variable slope (four parameters)" and the left-hand row gives the IC_{50} value in addition to standard error, and the R^2 value which is reflective of how well your data is within the bounds of the curve fit

3.5 Troubleshooting: Incomplete inhibition

Not all tested inhibitors will cause complete inhibition (integrated densities of 0 AU). Should this occur, the first step to take is increasing the concentrations of inhibitor evaluated. If the increased concentration range still does not yield full activity inhibition, GraphPad Prism enables a constraint to be set so that complete inhibition can be extrapolated. This likely should be the course of action if any issues arise with solubility of inhibitors at higher concentrations. When increasing the overall concentration of the dilution series, it may begin to be difficult to solubilize the inhibitor or the high concentrations could lead to colloidal aggregates of the compound itself or of the compound and protein. This potential aggregation can be checked with a native gel (see Section 3.6).

3.6 Troubleshooting: Inhibitor-induced protein aggregation

Protein aggregators, most often highly hydrophobic molecules, have previously been miscategorized as true HK inhibitors (Stephenson, Yamaguchi, & Hock, 2000). To differentiate specific inhibitors from aggregators, there are two effective methods. The first is to run a native gel with the suspected aggregator. Native gels contain no detergents and therefore can show aggregation through the loss of bands representing lower order protein oligomers, like monomers and dimers, and/or the appearance of higher bands representing higher order oligomers (Fig. 6). Proteins may run differently than expected on a native gel making controls essential. For HK853, aggregation can be observed through the loss of the dimeric protein band as the protein aggregates. A secondary option is to run the activity assay but remove TritonX-100 (follow identical protocol outlined in Section 3.3.2 skipping step 8). If significant changes in the IC_{50} value of the inhibitor are observed, it is likely that this compound is causing inhibition through aggregation rather than through a specific binding mode.

3.6.1 Native gel assay

3.6.1.1 Materials (in addition to those previously stated)

1. 50× Native Gel Running Buffer (7.5 g Tris, 36 g glycine, 250 mL MilliQ)
2. 20 mM HEPES Buffer (48 mg of HEPES in 10 mL of MilliQ water)
3. 7.5% native polyacrylamide gel

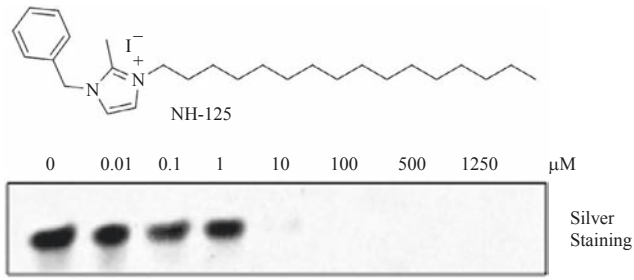

Fig. 6 Example native gel. At a range of concentrations of NH125, a known HK inhibitor, the dimer band of HK853 disappears by silver stain demonstrating the formation of aggregates and higher order oligomers. *Modified from: Goswami, M., Espinasse, A., Carlson, E. E. (2018). Disarming the virulence arsenal of* Pseudomonas aeruginosa *by blocking two-component system signaling.* Chemical Science, 10, *7332–7337. https://doi.org/10.1039/C8SC02496K.*

4. NH125 (Tocris Bioscience, cat #3439)—positive control for aggregation of HKs
5. DMSO—negative control for aggregation of HKs
6. Pierce Silver Stain Kit (ThermoFisher Scientific, cat #24612)

3.6.1.2 Protocol

1. Generated dilution series of inhibitor ranging from 20 to 25,000 μM (typically select 6 concentrations of inhibitors)

   Optional: include a positive control lane with NH125 > 10 μM, a known aggregator, and negative control lane with 0.5% v/v DMSO.
2. Thaw protein stock and exchanged it into 20 mM HEPES buffer and generate a 0.5 μM HK853 working stock solution (Section 3.3.2 steps 3–7, then 9)
3. Add working stock of HK853 (23.75 μL) into each sample tube
4. Add 1.25 μL of each inhibitor to reach a final reaction volume of 25 μL
5. Incubate protein and inhibitor for 30 min at RT
6. Add 8.6 μL of native-PAGE loading buffer to each sample
7. Load 15 μL of this sample onto a 7.5% polyacrylamide gel and ran with native gel running buffer for 1 h at 180 V
8. Remove gel from cassette and rinsed 3 × in MilliQ water
9. Stain with Pierce Silver Stain Kit following the manufacturers protocol
10. Scan in the Silver Stain channel

4. Concentration-dependent kinetics assay

4.1 Equipment

1. Micropipettors
2. Micropipette tips
3. 1.5 mL microcentrifuge tubes
4. Typhoon 9210 Gel Scanner (or similar model) with the following filters: Coomassie, ex/em 532 nm/570 nm ± 20 nm, BODIPY, ex/em 504 nm/514 nm ± 20 nm, TAMRA, ex/em 542 nm/568 nm ± 20 nm
5. Gel Electrophoresis Rig
6. Gel Rotator
7. Bench Top Centrifuge
8. Bench Top Vortex mixer
9. ImageJ software (NIH) for gel data analysis

4.2 Materials

1. Reaction Buffer (50 mM Tris-HCl, 200 mM KCl, 5 mM $MgCl_2$, pH 7.8)
2. ATPγS-BODIPY-FL (ThermoFisher, cat# A22184) or
3. ATPγNH-propargyl (Sigma-Aldrich, cat # 808512) or
4. ATPγO-propargyl (Jena Bioscience, cat # CLK-T10–1) or
5. ATPγS-propargyl (Espinasse, Wen, et al., 2020)
6. Triton X-100
7. Sodium dodecyl sulfate (SDS)
8. 10% Tris polyacrylamide gels
9. 4 × Loading Buffer [200 mM Tris-HCl, 400 mM dithiothreitol (DTT), 8% (*w*/*v*) Sodium dodecyl sulfate (SDS), 0.2% (w/v) bromophenol blue, 40% (*v*/v) glycerol, pH 6.8]
10. BenchMark™ Fluorescent Protein Standard (Invitrogen, cat# LC5928)
11. 10 × Tris-glycine SDS running buffer [144.0 g/L glycine, 30.0 g/L Tris, 10.0 g/L Sodium dodecyl sulfate (SDS); pH 8.3]
12. Coomassie brilliant blue R-250 staining solution (Bio-Rad, cat# 610436)
13. Gel-destaining solution (40% v/v acetic acid, 10% v/v methanol)

4.3 Protocol

Express and purify HK853 as described above, as well as exchanging it from storage buffer to reaction buffer (Sections 3.3.1 and 3.3.2, steps 4–12)

1. Vortex ATP probe stock of choice and generate a stock solution of 2000 μM probe
2. Generate a serial dilution of ATP probe of interest over the range of 20 μM to 1200 μM according to Table 2 for a total volume of 12 μL for each working probe stock, and vortex each sample well
3. Prepare a microcentrifuge tube for each [probe] sample and add reaction buffer (23.75 μL) to the tube
4. Make a 16.6 μM working stock of HK853
5. Vortex the HK853 working stock and add 1.50 μL of 16.6 μM HK853 into each microcentrifuge sample tube for a final protein concentration of 1 μM
6. Add 1.25 μL of each probe working stock to the appropriate tube for a final volume of 25 μL and a final probe range of 1–60 μM
7. Incubate at RT for 15 min (in the dark if using B-ATPγS)

Table 2 Probe working stock dilution series for gel-based concentration-dependent kinetics assay.

Previous working stock (μM)	Water to add (μL)	Previous working stock (μL)	Working stock (μM)	Final [probe] (μM)
40	6.00	6.00	20	1
100	7.20	4.80	40	2
200	6.00	6.00	100	5
400	6.00	6.00	200	10
900	5.33	6.67	500	25
1200	3.00	9.00	900	45
2000	4.80	7.20	1200	60

8. Quench reaction with a 10% (w/v) SDS, 10% Triton X-100 (v/v) solution in PBS (2.5 μL) for a final concentration of 1% SDS and 1% Triton X-100

If using propargyl probes continue to Section 5.1, if using B-ATPγS continue to next step.

9. Added 9 μL 4× loading buffer into each sample (*Stopping Point-freeze samples in loading buffer at −20°C*)
10. Run 10 μL of sample on a 10% polyacrylamide gel at 180 V for 1 h (Fig. 7)
11. Remove gel from cassette, rinse 3× with MilliQ water
12. Scan in BODIPY (ex/em 504 nm/514 nm ± 20 nm) or equivalent channel, then stain with 40 mL of Coomassie, microwave for 1 min, and rotate on gel shaker for 30 min
13. Remove Coomassie staining solution, rinse gel 3× with MilliQ water and add 40 mL of gel destaining solution, microwave again for 1 min
14. Let gel destain overnight and scan in Coomassie channel (ex/em 532 nm/570 nm ± 20 nm)

4.4 Analysis

1. Followed steps in Section 3.4.1
2. Calculate integrated densities from gel via steps 1–10 in Section 3.4.1
3. Using Graphpad Prism 8.0 (or similar software) plot each [probe] with its corresponding integrated densities serving as a proxy for enzyme activity, which in this case is the formation of the modified phosphohistidine species

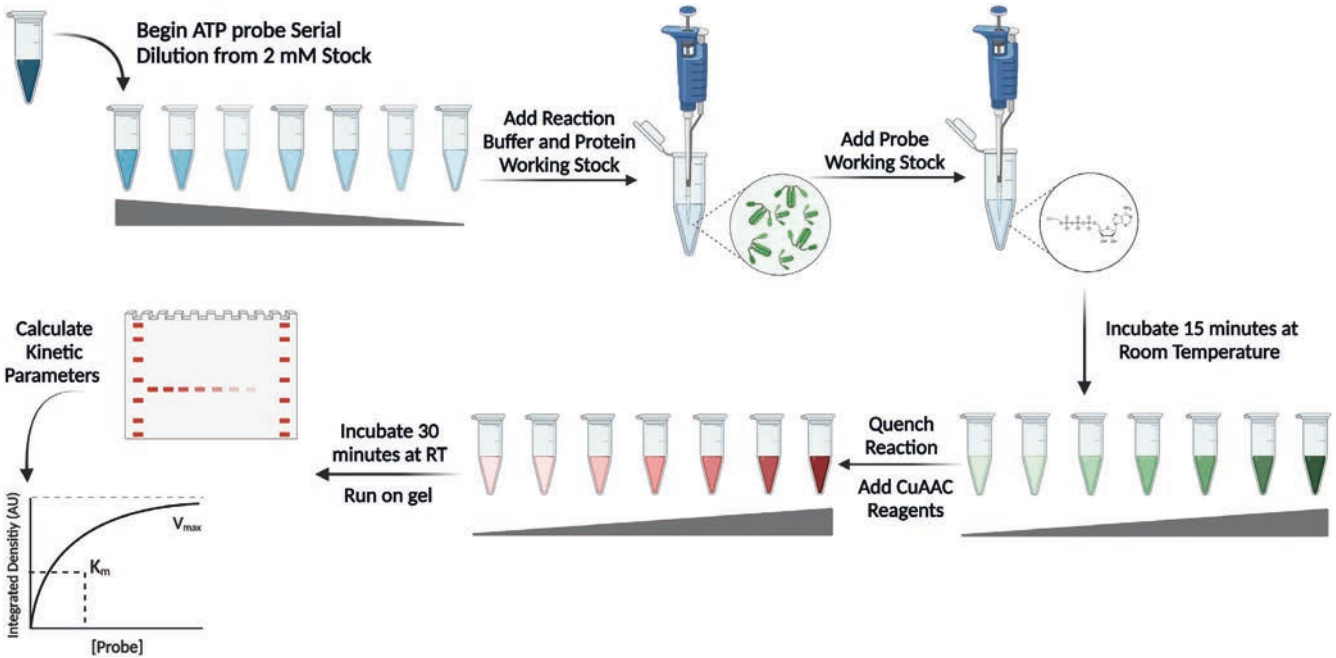

Fig. 7 Concentration-dependent kinetics assay schematic. From a dilution of the ATP probe stock, each concentration is incubated with HK853 for 15 min. Post-incubation the reaction is quenched with detergent and the CuAAC reagents are added and allowed to react for 30 min. After this, gel loading buffer is added, and each sample is run on a gel. The gel band intensities are quantified in ImageJ and kinetic parameters calculated in GraphPad Prism.

4. Biological replicates with their corresponding standard deviations can be included in the above data table
5. Select "New Analysis" and under the "XY Analyses" scroll to "Nonlinear Regression" title
6. Open "Enzyme Kinetics-Velocity as a function of substrate" from the equations set and select "k_{cat}"
7. Set the constraint for the programming, which is the concentration of enzyme catalytic sites (E_t). To do this, select the "Constrain" tab and ensure E_t has "Constant Equal to" and enter 25 for HK853 (25 μL of reaction volume/1 μM of HK853 in that reaction volume)
   7.1 If you do not know the value of E_t, you can calculate it by the reaction volume used in the assay over the concentration of protein present in that reaction volume. Otherwise, you can instead constrain to the V_{max} value. More information can be found in GraphPad's Curve Fitting Guide (GraphPad, 2021)
8. Under the "Results" tab, the "Nonlinear fit of Michaelis-Menten data" includes the calculated best fit values for k_{cat}, k_m, and V_{max}
9. The R^2 value can also be found under the "Results" tab describing how much variation the nonlinear curve is able to model from a given data set

4.5 Troubleshooting: Low signal intensity

Low signal intensity could be caused by various issues. If the protein of interest is only weakly active, a 15-min incubation may not be sufficient for a concentration-dependent assay. Instead, use a high concentration of probe and incubate with the desired protein for an increasing range of times. The labeling should be time dependent and then begin to saturate the enzyme active sites and yield consistent integrated band densities. Select a time point that gives strong and reliable signal and then maintain this time for the incubation step of the assay. If the fluorescent signal is high for a conjugated ATP probe such as B-ATPγS, but not the propargyl probes, then the CuAAC reaction is likely to blame. See Sections 5.4 and 5.5. If the labeling is low and the Coomassie stain is faint, or the integrated densities for the protein stain are similar to the fluorescent intensities, then the protein concentration is too low. Increase the amount of protein and maintain the same amount of probe until desired labeling is observed. Apply this protein concentration in future assays. If none of these strategies resolve the low intensities seen, the protein may not be able to utilize the substrate effectively. The use of fluorophore-conjugated probes can impact the activity of enzymes

(Fang et al., 2021), therefore using the ATP propargyl suite of probes could prove more effective. From here, ensure that aggregation is not occurring with the selected protein or probe concentration, a native gel should be run with the ATP probe of choice as described in Section 3.6. If the signal remains low after altering the time, the protein level, and the probe, change the range of the concentrations for the probe dilution series. Probe concentration can be increased if too little signal intensity is seen. If the intensities are high and stabilizing too quickly in the concentration series, reduce the concentration of the probe and the dilution series should be further diluted to parse out the kinetic parameters.

5. CuAAC reaction conditions

5.1 Equipment

1. Micropipettors
2. Micropipette tips
3. Typhoon 9210 Gel Scanner (or similar model) with the following filters: Coomassie, ex/em 532 nm/570 nm ± 20 nm, BODIPY, ex/em 504 nm/514 nm ± 20 nm, TAMRA, ex/em 542 nm/568 nm ± 20 nm
4. Gel Electrophoresis Rig
5. Gel Rotator
6. ImageJ software (NIH) for gel data analysis

5.2 Materials

1. TAMRA-PEG3-azide (BroadPharm, cat# BP22479) or any azide-functionalized fluorophore
2. Tris(2-carboxyethyl)phosphine (TCEP) (Sigma Aldrich, cat #C4706)
3. Tris((1-benzyl-4-triazolyl)methyl)amine (TBTA) (TCI Chemicals, cat# T2993)
4. Copper Sulfate $CuSO_4$
5. 10% Tris polyacrylamide gels
6. 4 × Loading Buffer [200 mM Tris-HCl, 400 mM dithiothreitol (DTT), 8% (*w*/*v*) SDS, 0.2% (w/v) bromophenol blue, 40% (*v*/v) glycerol, pH 6.8]
7. BenchMark™ Fluorescent Protein Standard (Invitrogen, cat# LC5928)
8. 10 × Tris-glycine SDS running buffer (144.0 g/L glycine, 30.0 g/L Tris, 10.0 g/L SDS; pH 8.3)

9. Coomassie brilliant blue R-250 staining solution (Bio-Rad, cat #1610436)
10. Gel-destaining solution (40% v/v acetic acid, 10% v/v methanol)

5.3 Protocol

1. Made fresh a 5 mM working stock solution of TAMRA azide
2. Made fresh a 50 mM working stock solution of TCEP
3. Made fresh a 10 mM working stock solution of TBTA
4. Made fresh a 50 mM working stock solution of $CuSO_4$

It is critical that the reaction components be added in the following order:

5. Azide fluorophore (1 μL) was added to the sample tube (29 μL) for a final concentration of 0.16 mM
6. Then add TCEP (0.8 μL) for a final concentration of 1.3 mM, followed by TBTA (0.4 μL) for a final concentration of 0.13 mM
7. Lastly add $CuSO_4$ (0.8 μL) for a final concentration of 1.3 mM. Incubate solution with all CuAAC reaction components for 30 min at RT
8. Add 10 μL of 4 × loading buffer (*Stopping Point-freeze samples in loading buffer at* $-20°C$)
9. Run 10 μL of sample on a 10% polyacrylamide gel at 180 V for 1 h in the dark on ice
10. Remove gel from cassette, rinse 3 × with MilliQ water
11. Scan in TAMRA (ex/em 542 nm/568 nm ± 20 nm) or equivalent channel, then stain gel with 40 mL of Coomassie, microwave for 1 min, and rotate on gel shaker for 30 min
12. Remove Coomassie stain, rinse gel 3 × with MilliQ water and add 40 mL of gel destaining solution and microwave again for 1 min
13. Let gel destain overnight and scan in Coomassie channel (ex/em 532 nm/570 nm ± 20 nm).

5.4 Troubleshooting: High background in CuAAC gels

High background can make band intensity difficult to measure and is often caused by excess click reagents causing low level fluorescence "streaking" throughout a lane. To rid your sample of this contamination, add a protein precipitation step using a Proteo extract kit following the manufacturer's protocol. Reducing the concentration of all click reagents or incubation time can also help to reduce non-specific labeling or high background.

5.5 Troubleshooting: Low CuAAC efficiency

There are many reasons for low fluorescence intensity in a CuAAC gel. First, ensure that all stocks of the CuAAC reagent are made fresh immediately prior to the reaction. Fluorophores can handle freeze-thaw cycles, but best practice is still to aliquot these stocks to minimize the freeze-thaw cycles that they undergo. For all other reagents needed, do not keep stock solutions as degraded reagents may cause lowered reactivity. Additionally, low labeling from a CuAAC reaction could be due to poor accessibility of the probe within the enzyme active site. To discern if labeling site availability may be causing inefficient labeling, test the CuAAC reaction under denaturing conditions to see if this enables better exposure of the bioorthogonal group to the CuAAC reagents. If increased labeling is seen under denaturing conditions, it is likely that probe accessibility is to blame. However, if low labeling persists experiments should be performed to ensure that the probe is labeling the protein itself if they have not already been completed.

6. Conclusion

Within chemical biology, ABPs are key to understanding enzyme activity at various timepoints and under varying conditions. Further development of ABPs will continue to close fundamental knowledge gaps. The use of ATP-based ABPs is particularly impactful given their versatility in cells. While we have previously demonstrated the utility of these probes to determine key kinetic parameters, in addition to evaluating the potency of putative inhibitors, their use extends far past these two examples. While our work focuses on the HKs, this suite of ATP-based ABPs are powerful tools for the study of other ATP-binding proteins including evaluation of their activity, catalytic efficiency, and level of inhibition.

Acknowledgments

This work was funded by the NSF (CHE-2003208) and the UMN Office of Academic Clinical Affairs. H.K.L. is funded by the UMN NIH Biotechnology Training Grant 5T32GM008347-30. Images made in BioRender. We thank Conrad A. Fihn for helpful comments.

References

Albanesi, D., Martín, M., Trajtenberg, F., Mansilla, M. C., Haouz, A., Alzari, P. M., et al. (2009). Structural plasticity and catalysis regulation of a thermosensor histidine kinase. *PNAS*, *106*(38), 16185–16190.

Beier, D., & Gross, R. (2006). Regulation of bacterial virulence by two-component systems. *Current Opinion in Microbiology*, *9*(2), 143–152.

Bem, A. E., Velikova, N., Pellicer, M. T., Baarlen, P., Marina, A., & Wells, J. M. (2015). Bacterial histidine kinases as novel antibacterial drug targets. *ACS Chemical Biology*, *10*(1), 213–224.

Bhagirath, A. Y., Li, Y., Patidar, R., Yerex, K., Ma, X., Kumar, A., et al. (2019). Two component regulatory systems and antibiotic resistance in gram-negative pathogens. *International Journal of Molecular Sciences*, *20*(7).

Cannistraro, V. J., Glekas, G. D., Rao, C. V., & Ordal, G. W. (2011). Cellular stoichiometry of the chemotaxis proteins in Bacillus subtilis. *Journal of Bacteriology*, *193*(13), 3220–3227.

Casino, P., Miguel-Romero, L., & Marina, A. (2014). Visualizing autophosphorylation in histidine kinases. *Nature Communications*, *5*(1), 3258.

Coleman, N., Nguyen, H. M., Cao, Z., Brown, B. M., Jenkins, D. P., Zolkowska, D., et al. (2015). The riluzole derivative 2-amino-6-trifluoromethylthio-benzothiazole (SKA-19), a mixed KCa2 activator and NaV blocker, is a potent novel anticonvulsant. *Neurotherapeutics*, *12*(1), 234–249.

Dommerholt, J., van Rooijen, O., Borrmann, A., Guerra, C. F., Bickelhaupt, F. M., & van Delft, F. L. (2014). Highly accelerated inverse electron-demand cycloaddition of electron-deficient azides with aliphatic cyclooctynes. *Nature Communications*, *5*(1), 5378.

Dorr, T., Alvarez, L., Delgado, F., Davis, B. M., Cava, F., & Waldor, M. K. (2016). A cell wall damage response mediated by a sensor kinase/response regulator pair enables beta-lactam tolerance. *Proceedings of the National Academy of Sciences of the United States of America*, *113*(2), 404–409.

Espinasse, A., Lembke, H. K., Cao, A. A., & Carlson, E. E. (2020). Modified nucleoside triphosphates in bacterial research for in vitro and live-cell applications. *RSC Chemical Biology*, *1*, 333–351.

Espinasse, A., Wen, X., Goodpaster, J. D., & Carlson, E. E. (2020). Mechanistic studies of bioorthogonal ATP analogues for assessment of histidine kinase autophosphorylation. *ACS Chemical Biology*, *15*(5), 1252–1260.

Fang, H., Peng, B., Ong, S. Y., Wu, Q., Li, L., & Yao, S. Q. (2021). Recent advances in activity-based probes (ABPs) and affinity-based probes (AfBPs) for profiling of enzymes. *Chemical Science*, *12*(24), 8288–8310.

Francis, V. I., Stevenson, E. C., & Porter, S. L. (2017). Two-component systems required for virulence in Pseudomonas aeruginosa. *FEMS Microbiology Letters*, *364*(11), fnx104.

Goswami, M., Espinasse, A., & Carlson, E. E. (2018). Disarming the virulence arsenal of Pseudomonas aeruginosa by blocking two-component system signaling. *Chemical Science*, *9*(37), 7332–7337.

Gotoh, Y., Eguchi, Y., Watanabe, T., Okamoto, S., Doi, A., & Utsumi, R. (2010). Two-component signal transduction as potential drug targets in pathogenic bacteria. *Current Opinion in Microbiology*, *13*(2), 232–239.

GraphPad. (2021). *Prism 8 Curve Fitting Guide*. From https://www.graphpad.com/guides/prism/8/curve-fitting/index.htm.

Hazelbauer, G. L., & Lai, W. C. (2010). Bacterial chemoreceptors: Providing enhanced features to two-component signaling. *Current Opinion in Microbiology*, *13*(2), 124–132.

Heal, W. P., Dang, T. H., & Tate, E. W. (2011). Activity-based probes: Discovering new biology and new drug targets. *Chemical Society Reviews*, *40*(1), 246–257.

Hong, V., Presolski, S. I., Ma, C., & Finn, M. G. (2009). Analysis and optimization of copper-catalyzed azide-alkyne cycloaddition for bioconjugation. *Angewandte Chemie International Edition*, *48*(52), 9879–9883.

Kee, J. M., & Muir, T. W. (2012). Chasing phosphohistidine, an elusive sibling in the phosphoamino acid family. *ACS Chemical Biology*, *7*(1), 44–51.

Li, M., & Hazelbauer, G. L. (2004). Cellular stoichiometry of the components of the chemotaxis signaling complex. *Journal of Bacteriology*, *186*(12), 3687–3694.
Makwana, M. V., Muimo, R., & Jackson, R. F. (2018). Advances in development of new tools for the study of phosphohistidine. *Laboratory Investigation*, *98*(3), 291–303.
Marina, A., Waldburger, C. D., & Hendrickson, W. A. (2005). Structure of the entire cytoplasmic portion of a sensor histidine-kinase protein. *The EMBO Journal*, *24*(24), 4247–4259.
Matthews, M. L., He, L., Horning, B. D., Olson, E. J., Correia, B. E., & Yates, J. R. (2017). Chemoproteomic profiling and discovery of protein electrophiles in human cells. *Nature Chemistry*, *9*(3), 234–243.
Muller, S., Gotz, M., & Beier, D. (2009). Histidine residue 94 is involved in pH sensing by histidine kinase ArsS of helicobacter pylori. *PLoS One*, *4*(9), e6930.
NIH. (2021). *ImageJ image processing and analysis in Java*. From https://imagej.nih.gov/ij/download.html.
Shamshurin, D., Krokhin, O. V., Levin, D., Sparling, R., & Wilkins, J. A. (2014). In situ activity-based protein profiling of serine hydrolases in E. coli. *EuPA Open Proteomics*, *4*, 18–24.
Sharifzadeh, S., Shirley, J. D., & Carlson, E. E. (2019). *Activity-based protein profiling methods to study bacteria: The power of small molecule electrophiles*. Berlin: Springer.
Stephenson, K., Yamaguchi, Y., & Hock, J. A. (2000). The mechanism of action of inhibitors of bacterial two-component signal transduction system. *Journal of Biological Chemistry*, *275*, 38900–38904.
Stock, A. M., Robinson, V. L., & Goudreau, P. L. (2000). Two component signal transduction. *Annual Review of Biochemistry*, *69*, 183–215.
Surette, M. G., Levit, M., Liu, Y., Lukat, G., Ninfa, E. G., Ninfa, A., et al. (1996). Dimerization is required for the activity of the protein histidine kinase CheA that mediates signal transduction in bacterial chemotaxis. *The Journal of Biological Chemistry*, *271*, 939–945.
Wang, S., Tian, Y., Wang, M., Wang, M., Sun, G. B., & Sun, X. B. (2018). Advanced activity-based protein profiling application strategies for drug development. *Frontiers in Pharmacology*, *9*, 353.
Wilke, K. E., Francis, S., & Carlson, E. E. (2012). Activity-based probe for histidine kinase signaling. *Journal of the American Chemical Society*, *134*(22), 9150–9153.
Wilke, K. E., Francis, S., & Carlson, E. E. (2015). Inactivation of multiple bacterial histidine kinases by targeting the ATP-binding domain. *ACS Chemical Biology*, *10*(1), 328–335.
Wright, M. H., & Sieber, S. A. (2016). Chemical proteomics approaches for identifying the cellular targets of natural products. *Natural Product Reports*, *33*(5), 681–708.
Zanon, P. R. A., Lewald, L., & Hacker, S. M. (2020). Isotopically labeled Desthiobiotin Azide (isoDTB) tags enable global profiling of the bacterial Cysteinome. *Angewandte Chemie (International Ed. in English)*, *59*(7), 2829–2836.